23rd ABCM International Congress of Mechanical Engineering
December 6-11, 2015, Rio de Janeiro, RJ, Brazil

COMPUTATIONAL FLUID DYNAMICS APPLIED TO JET PUMPS

Michele C. Pedroso (*)
Universidade Estadual de Campinas (UNICAMP)
m.pedroso@petrobras.com.br
(*) now at PETROBRAS/ R&D Center (CENPES)

Antonio C. Bannwart
Universidade Estadual de Campinas (UNICAMP), Faculdade de Engenharia Mecânica, Departamento de Engenharia de Petróleo.
Rua Mendeleiev, 200 – Cidade Universitária/Barão Geraldo – CEP:13.083-860 – Campinas (SP)
bannwart@dep.fem.unicamp.br

Rigoberto E. M. Morales
Universidade Tecnológica Federal do Paraná (UTFPR), Departamento Acadêmico de Mecânica – DAMEC.
Av. Sete de Setembro, 3165 – Rebouças – CEP: 80.230-901 – Curitiba (PR)
rmorales@ utfpr.edu.br

Elisio F. Caetano
PETROBRAS/ R&D Center (CENPES)
Av. Horácio Macedo, 950 – Ilha do Fundão – CEP: 21.941-150 – Rio de Janeiro (RJ)
ecaetano@petrobras.com.br

Abstract. *This article presents a two-dimensional computational fluid dynamic (CFD) study applied to a set of sixteen different geometries of jet pumps, where water is the power fluid (primary) and also the moved fluid (secondary), which is commonly called liquid Jet Liquid Pump (LJL). The numerical CFD methodology of analysis was validated by experimental data from the literature, revealing good agreement between CFD and experimental results, with a deviation of less than 5% for the pump capacity ratio at the maximum efficiency spot. The CFD study, for the proposed geometries, allowed knowing the influence on pump efficiency of the typical design parameters (1) nozzle-to-throat area ratio and, (2) the throat length. The results showed that the (1) nozzle-to-throat area ratio strongly defines the pumping mass range capacity, while the optimization of (2), the throat length, considerably defines the pump efficiency. The good results obtained with the developed methodology, when applied to water jet pumps, seem to indicate that such methodology might as well be potentially applied to jet pumps where the primary fluid is a liquid hydrocarbon and the secondary a gas and/or a gas-liquid hydrocarbon mixture – provided that proper modelling treatment for those particular types of fluids and flows be incorporated into the methodology.*
Keywords: *Jet Pump, Ejector, Liquid Jet Liquid, Hydraulic Jet Pump, Injector.*

1. INTRODUCTION

An ejector, eductor, injector, jet pump, jet compressor or siphon are just different types of an ejector function of the used fluids and existent flow conditions. Its structural simplicity, absence of moving parts and easy maintenance have made this pump concept to be widely used in many fields for several purposes, such as moving liquid, gas, liquid-gas mixtures, steam and even solids (Jumpeter, 2008).

The ejector works by Venturi's effect, which is a particular case of the Bernoulli's principle. Basically, fluid (primary) under pressure is converted into a high-velocity jet at the outlet of a convergent nozzle which creates a low pressure at that point. In essence, the pressure energy of the inlet motive fluid is converted to kinetic energy in the form of velocity head at the convergent nozzle outlet. The low pressure draws the suction fluid (secondary) into the ejector throat where it mixes with the motive fluid. The mixed fluid then expands inside the divergent diffuser, thus recovering pressure. As the mixed fluid then expands inside the divergent diffuser, the kinetic energy is converted back to pressure energy at the diffuser outlet in accordance to the Bernoulli's principle – needless to say, irreversibility effects are also present in these energy conversions.

The liquid-liquid ejectors have been extensively studied and it is a well-known fact that nozzle-to-throat ratio, throat length and nozzle-to-throat distance are the main geometrical parameters in the modelling and design of ejectors. In the experimental study of Sanger (1970), several geometries of low values of nozzle-to-throat area ratios are investigated. Cunningham (1970) investigates the cavitation phenomenon on these liquid-liquid ejectors. Cunningham's one-dimensional model (1995) has been widely used in the efficiency analysis and design of this type of ejector. However, none of those models were deemed able to properly predict the behaviour of ejectors by themselves, since the energy losses along the flow inside such devices are not captured. Lima Neto (2011), theoretically and experimentally investigated the maximum suction lift of water jet pumps with different nominal diameters and nozzle-to-throat area ratios. In his study, dimensionless correlations to describe the maximum suction lift for the non-cavitation region and to predict the onset of such phenomenon were derived.

In the petroleum industry, the use of ejectors is well-established and they are more often referred to as jet pumps. A typical application in well production is the artificial lift method known as Hydraulic Jet Pump (Fretweel, 2006). The liquid-liquid ejectors can be used in wells but, preferably, with no gas presence. Liquid Jet Gas Liquid ejectors (LJGL) such as the ones used to move liquid-gas mixtures can also be used as oil industry equipment, notwithstanding its higher complexity when compared to a LJL pump. Cunningham (1995) also presents a one-dimensional model for a Liquid Jet Gas Liquid (LJGL) ejector developed apart from experimental data. Baohua (1985) presents a study for LJGL, making experimental usage of a particular and commercially available jet pump concept, from which he presented a model to estimate the efficiency of such type of jet pump. Noronha *et al* (1998) proposed an improved model to estimate the efficiency of LJGL pumps, and offered comparisons with the Baohua's model, showing better fits for the same experimental results.

In summary, during the development of this study, no comprehensive modelling of the liquid-liquid ejector's behaviour was identified in the literature. The lack of comprehensiveness is a characteristic of all one-dimensional models since they all need the previous knowledge about the energy loss coefficients in order to predict the respective pump flow efficiency. In recent years, the technique known as Computational Fluid Dynamics (CFD) has become an approach often used in studies and design of ejectors due to its lower cost and good reliability when compared to experimentation. Yapici and Aldas (2013) adopted the CFD in the study of six water jet pumps with different nozzle-to-throat area ratios. The results were compared with experimental data provided by the literature and a maximum deviation value of approximately 10% for the pump efficiency at the optimum operating conditions was reported. Cruz (2006) adopted a three-dimensional discretization model in his CFD analysis of a jet pump, which resulted in more than one million volume elements in the respective flow domain. The results showed good agreement with the experimental data, at a highly time-consuming mesh however. It has also been found that the majority of the numerical studies were performed under a three-dimensional coverage of the flow domain volume. Such approach ended up requiring very large meshes and, consequently, higher computational costs during the studies as well. Thus, whenever advisable, the usage of two-dimensional discretization approach provides advantages, as such approach can be easily implemented, generating a much smaller number of volume elements and also allowing a huge reduction in the computational time required when compared with the three-dimension discretization approach.

In the present study, a two-dimensional modelling making usage of a commercial CFD package (Ansys, 2013a, 2013b) combined with selected boundary conditions, turbulence model and a discretization scheme of the flow field was conceived. Liquid jet liquid pumps were studied by using such methodology, which has been validated with experimental data (Sanger, 1970). It is believed that such methodology, by being simple and able to generated fast results, contributes to the analysis and design of these pumps. This phase of the ongoing study is reported herein.

2. MATHEMATICAL MODELING

2.1 Liquid Jet Liquid Pump Equations

Some dimensionless parameters are useful for the understanding and comparisons related to the efficiency of LJL pumps. Amongst those, the most typical ones are: (1) nozzle-to-throat area ratio; (2) the mass flow ratio; (3) the produced head; and (4) the efficiency. The nozzle-to-throat area ratio is defined as:

$$b = \frac{A_n}{A_{th}} \tag{1}$$

Where A_n is the convergent nozzle terminal area and, A_{th} is the throat area – typically constant along its length. The efficiency η is defined as the ratio of useful work rate on the secondary fluid to the energy extracted from the primary fluid:

$$\eta = \frac{(P_d - P_s) * Q_2 * \rho_2}{(P_i - P_d) * Q_1 * \rho_1} = H * M \tag{2}$$

Where Q_2 is the volumetric flowrate of the secondary fluid and, Q_1 is the volumetric flow rate of the primary fluid. And, ρ_1 is the volumetric mass density of the primary fluid and, ρ_2 is the volumetric mass density of the secondary fluid. P_d is the discharge pressure for the mixture, P_s is the pressure of the secondary fluid at its inlet spot and, similarly, P_i is the pressure of the primary fluid at the inlet spot. M is the $\rho_2 Q_2/\rho_1 Q_1$ ratio, termed as Mass Flowrate Ratio. H is termed as Dimensionless Head.

Cavitation is an important phenomenon to be considered when trying to evaluate the behavior of jet pumps. The cavitation is the formation of gas bubbles of a flowing liquid and, it happens in a region where the local pressure value drops below the vapor pressure for such flowing liquid. Upon cavitation, any reduction in the system back pressure has no effect on the flow. The occurrence of such phenomenon is avoided whenever the so-called cavitation-limited flow ratio condition (M_L) is not reached. A wide set of cavitation models can be found in Cunningham *et al* (1970). In this work, the Cunningham model is used to predict the onset of cavitation limited by flow, which is defined as:

$$M_L = \frac{1-b}{b}\sqrt{\frac{(P_d \quad P_v)}{(\sigma_L)*Z}} \tag{3}$$

Where P_v is the vapour pressure of the primary fluid, (σ_L) is a constant and Z is the jet dynamic pressure. In the next section, the complete set of equations that describes the behaviour of a compressible Newtonian fluid flow is presented.

2.2 Mathematical equations

The equations required to evaluate an isothermal Newtonian fluid flow are the continuity and the momentum balance equations. In addition, a turbulence model (to handle the chaotic characteristic of the flow) is also required.

The continuity equation is given by the mass balance in one volume element (Bird, 2002):

$$\frac{\partial \rho}{\partial t} + [\nabla . \rho \boldsymbol{v}] = 0 \tag{4}$$

The momentum balance equation is given by (Bird, 2002):

$$\frac{\partial \rho \boldsymbol{v}}{\partial t} = -[\nabla . \rho \boldsymbol{v}\boldsymbol{v}] - \nabla p - [\nabla . \boldsymbol{\tau}] + \rho \boldsymbol{g} \tag{5}$$

Where $\boldsymbol{\tau}$ is the relation for the stresses in a Newtonian fluid flow.

2.3 The Turbulence Model

The turbulence model used in the present study is the κ-ε standard model (Launder & Spalding, 1973). Such model is a two-equation turbulence model where the velocity and the length scale are both solved using separate transport equations. This method is widely used and was chosen due to its numerical robustness and has a well-established regime of predictive capability. Two important variable definitions are given by this model. The first one is the turbulent kinetic energy κ and, the second one is the rate of viscous dissipation, ε.

The momentum equation is written as (Ansys, 2013a):

$$\frac{\partial \rho v_i}{\partial t} + \frac{\partial (\rho v_i v_j)}{\partial x_j} = -\frac{\partial P'}{\partial x_i} + \frac{\partial}{\partial x_j}\left[\mu_{eff}\left(\frac{\partial v_i}{\partial x_j} - \frac{\partial v_j}{\partial x_i}\right)\right] + S_M \tag{6}$$

Where S_M represents the sum of the body forces, P´ is the modified pressure (Eq. 7) and μ_{eff} is the effective viscosity (Eq. 8), which considers turbulence effects due to turbulent viscosity ($\mu_t = C_\mu \rho \frac{\kappa^2}{\varepsilon}$); C_μ is a constant.

$$P' = P + \frac{2}{3}\rho\kappa + \frac{2}{3}\mu_{eff}\frac{\partial v_i}{\partial x_i} \tag{7}$$

$$\mu_{eff} = \mu + C_\mu \rho \frac{\kappa^2}{\varepsilon} \tag{8}$$

The κ-ε standard model uses the following equations for the transport of κ and ε (Ansys, 2013a),

$$\frac{\partial (\rho\kappa)}{\partial t} + \left[\frac{\partial (\rho v_j \kappa)}{\partial x_j}\right] = \frac{\partial}{\partial x_j}\left[\left(\mu + \frac{\mu_t}{\sigma_\kappa}\right)\frac{\partial \kappa}{\partial x_j}\right] + P_\kappa - \rho\varepsilon + P_{\kappa b} \tag{9}$$

$$\frac{\partial (\rho\varepsilon)}{\partial t} + \left[\frac{\partial (\rho v_j \varepsilon)}{\partial x_j}\right] = \frac{\partial}{\partial x_j}\left[\left(\mu + \frac{\mu_t}{\sigma_\varepsilon}\right)\frac{\partial \varepsilon}{\partial x_j}\right] + \frac{\varepsilon}{\kappa}\left(C_{\varepsilon 1}P_\kappa - C_{\varepsilon 2}\rho\varepsilon + C_{\varepsilon 1}P_{\varepsilon b}\right) \tag{10}$$

Where, $C_{\varepsilon 1}, C_{\varepsilon 2}$, σ_ε and σ_κ are constants. $P_{\kappa b}$ and $P_{\varepsilon b}$ are related to the buoyance forces. P_κ is the turbulence production due to viscous forces.

Boundary conditions are required for a complete description of the flow field inside these pumps. They are: (1) the wall boundary; (2) the plane of symmetry; (3) the inlet flow conditions and (4) the outlet flow conditions. The no-slip and non-permeable wall boundary conditions require velocities equal to zero along the wall. The symmetry-plane boundary condition requires the normal velocity equal to zero and the scalar variable gradients, normal to the boundary, being also equal to zero. The inlet and outlet boundaries are discussed along the text.

3. METHODOLOGY

3.1 Finite Volume Discretization Method

ANSYS CFX (Ansys, 2013a) was the software used to predict the flow field characteristics in a jet pump, by solving the set of pertinent equations presented in the former section. This software uses an element-based finite volume method. The basic idea of finite volume method is to discretize the flow domain into a set of control volumes. The equations of mass flow balance (continuity), momentum and energy are discretized and solved iteratively for each control volume.

The ejectors here studied are axially symmetric, which allows the use of a two-dimensional mesh. The actual geometry of the ejector is defined in the CFX Solver by using a boundary condition termed as symmetry plane. In addition, the assumption of an isothermal flow allows the energy balance to be disregarded.

The CFD results must be independent of the selected mesh. So it is necessary to try different refinement to the mesh until the results do not change significantly – process termed as mesh test. The mesh refinement is a balance between the computational time needed for the simulation and the needs of the adopted description model. After the referred mesh test, the chosen and the adopted mesh for the modelling of the LJL used in the Sanger's experiments amounted to approximately 46,000 elements of volume.

All the simulations require the control of the variable Y^+ near a specific range. The Y^+ is the dimensionless distance from the wall and it is used to check the location of the first simulation node away from the wall. This quantity is important when wall functions are used to describe the turbulent boundary layer, which is the case here. The κ-ε standard model suggests a rule-of-thumb of keeping the Y^+ value between 20~30 for the wall region in which the high Reynolds numbers are found – in jet pumps, such wall region is the one in the convergent nozzle outlet.

3.2 Validation

In order to validate the suitability of the developed methodology, comparisons with experimental data are required. Thus, the literature search initially brought forward the results obtained by Sanger (1970). Such investigator worked with LJL pumps (water jet pumps) having a nozzle-to-throat area ratio, *b*, equal to 0.066, a throat length, *L*, equal to 5.66 throat diameters and, a nozzle-to-throat distance (NTD) equal to zero. The two-dimensional mesh was built by the ICEM software (Ansys, 2013b). The Fig. 1 shows the geometry used by Sanger (1970).

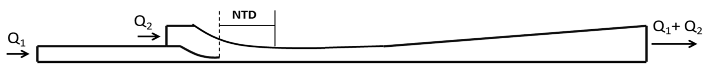

Fig. 1 – Sanger's experimented LJL pump geometry - schematic view

All simulations were carried out according to the range of operational values proposed by Sanger (1970). The reported experimental operational conditions were: P_s = 0 Pa; Q_1=1.762x10^{-3} m^3/s; and *M* varying within the 0.92 to 5.39 range. Thus, the CFD boundary conditions were set as: the suction pressure for the secondary fluid (constant); the mass flow rate of the primary fluid (constant); and the mass flowrate of the mixture in the divergent nozzle outlet (always variable). The walls were considered smooth, the flow isothermal and at a constant temperature of 298.16 K.

3.3 CDF Two-dimensional Results Validation

The jet pump efficiency, *η*, and the dimensionless head, *H*, curves are presented in the Fig. 2 and Fig. 3 respectively as function of the mass flowrate ratio (*M*). The curves show the experimental data of Sanger (1970) and the results presented by the developed methodology based on the CFD approach.

The comparison showed a good agreement between CFD and experimental results, with a deviation of less than 5% for the pump capacity ratio at the point of maximum efficiency. Fig. 2 shows the deviation between the CFD prediction and the experimental results for the upper values of the mass flowrate ratio (*M*). An explanation for such behaviour might relate to the adopted turbulence κ-ε standard model. This model, which is widely used for internal flows despite being regarded as an effective turbulence model for engineering flows (Nallasamy, 1985), is also considered as not sufficiently suitable to describe round jets. Such weakness might be explained on the grounds of the "round jet anomaly" of the κ-ε standard model which, typically, predicts that the round jet spreads 40% faster than it really does, while plane jet velocity fields are calculated quite accurately, as found by Pope (1978). According to Yule *et al* (1993), the standard κ-ε model exhibits errors in the prediction of piped jets that are similar to those found in earlier studies of round free jets. Thus, the κ-ε standard model by over predicting the jet spreading out action, ends up over predicting the mixture process between the primary and secondary fluid flows inside the ejector's throat region. The result is a prediction of a more homogeneous velocity profile in the throat outlet, which will lead to a pressure recovery level inside the ejector's diffuser region that is higher than the experimentally observed. Such overestimated pressure recovery level leads to the equally observed over prediction efficiency for the studied jet pump.

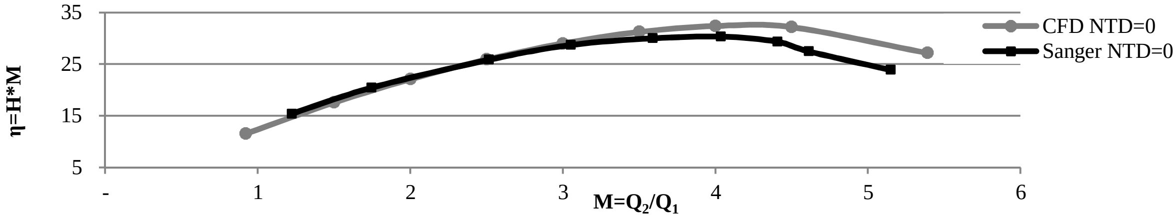

Fig. 2 – Sanger's (1970) LJL efficiency (η) - experimental versus CFD results

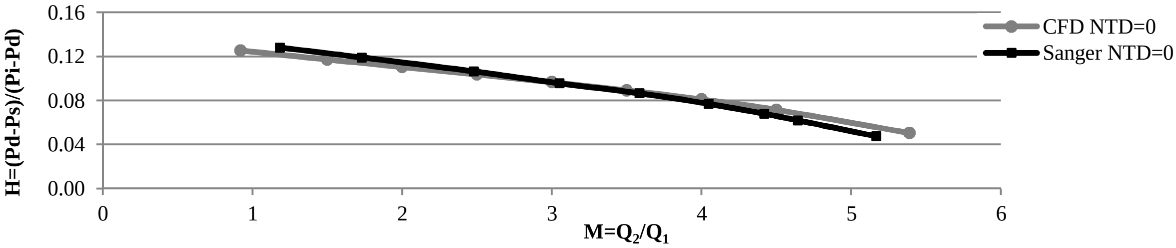

Fig. 3 – Sanger's (1970) LJL dimensionless Head (H) - experimental versus CFD results

The adopted cavitation limit model as described in the Eq. 3 was applied to the Sanger geometry and associated experimental data set. Such application resulted in the value 5.9 for the M_L parameter, which confirmed the non-occurrence of such phenomenon in such data set as can be observed in Fig. 2 and 3.

4. CASE STUDIESES AND RESULTS

The studied LJL geometries were the ones resulting from the dimensions given in Fig. 4. As following presented, several CFD analysis were performed and the found three more interesting Case Studies ones are here reported.

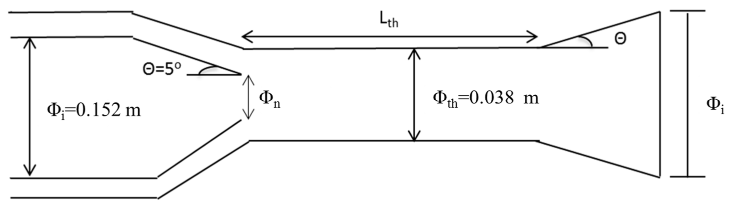

Fig. 4 – Jet Pump: overall geometry (out of scale) composing the studied cases

The Case Studies #1 and #2 are composed by a set of seven and three different geometries respectively. The geometrical parameters are shown in Tab. 1. The main objective of the Case Study #1 was to understand the influence of the nozzle-to-throat area ratio in the jet pump efficiency. The main objective of Case Study #2 was to verify the influence of the mixing throat length in the jet pump efficiency.

Table 1 – Jet Pump Parameters of Study - Case #1 and Case #2

Study Case #1				**Study Case #2**			
	b	**Φ_n (10^{-2} m)**	**L_{th}**		**b**	**Φ_n (10^{-2} m)**	**L_{th}**
Geom1	0.15	1.46	$10\Phi_{th}$	Geom8	0.25	1.88	$20\Phi_{th}$
Geom2	0.20	1.68	$10\Phi_{th}$	Geom9	0.30	2.06	$20\ \Phi_{th}$
Geom3	0.25	1.88	$10\Phi_{th}$	Geom10	0.35	2.23	$20\ \Phi_{th}$
Geom4	0.30	2.06	$10\Phi_{th}$				
Geom5	0.35	2.23	$10\Phi_{th}$				
Geom6	0.40	2.38	$10\Phi_{th}$				
Geom7	0.55	2.79	$10\Phi_{th}$				

The primary and secondary fluids were both water. The boundary conditions were: the primary and the secondary fluid pressures and the total mass flow rate at the outlet. The primary fluid pressure was set to 70 barg and the total mass flow rate in the outlet was set to 30 kg/s for all simulated conditions. The secondary fluid intake pressure varied within a defined range of values. Such range was estimated when the geometry was considered to be only the ejector's convergent nozzle region. Every efficiency curve is a set of several simulations with different secondary fluid inlet pressure values.

The Fig. 5 shows the efficiency curves that resulted from the CFD analysis performed for the jet pump geometries composing the Case Study #1. According to Cunningham (2008), comparisons of *b*-value series of pumps show that peak efficiency is highest for *b* in the 0.2 to 0.3 range. The studied geometries showed the same trend values, where it can be seen that the maximum efficiency value is achieved for the nozzle-to-throat area ratio equal to 0.30.

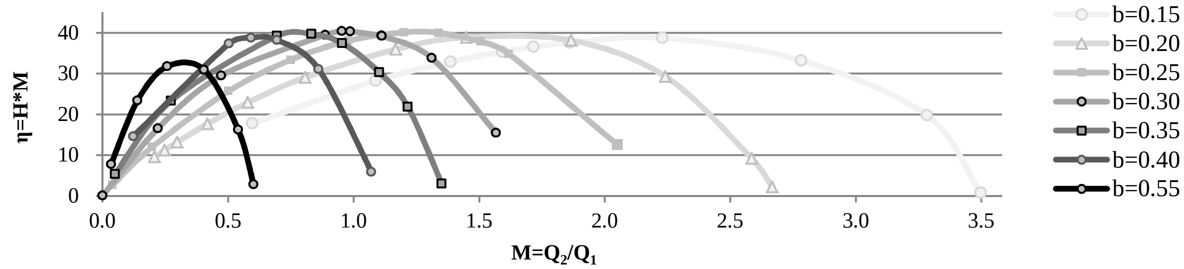

Fig.5 – Case Study #1 – Efficiency curves (η) as a function of the nozzle-to-throat area ratio

The Fig. 6 presents the dimensionless head curves for the seven jet pump geometries imbedded in the aforementioned Case Study #1. Another result that can be drawn from this analysis is that the lower the nozzle-to-throat area ratio (*b*) value, the wider the pump capacity range in terms of mass flowrate ratio (*M*) and the lower the dimensionless head available (*H*).

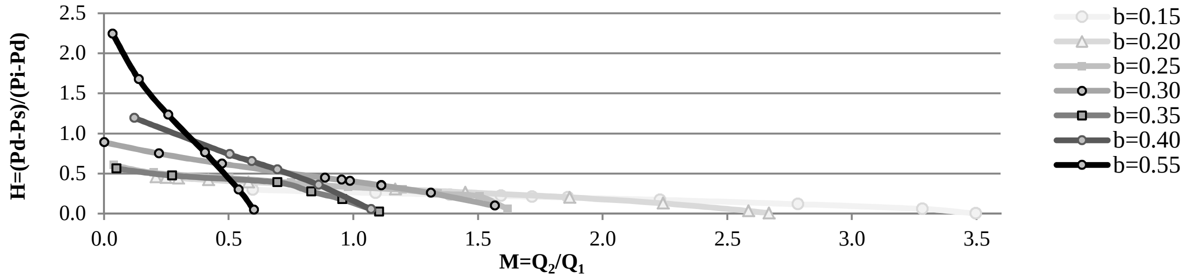

Fig. 6 – Case Study #1 – Dimensionless head curves (*H*) as a function of the nozzle-to-throat area ratio

Fig. 7 shows the efficiency curves that resulted from the CFD analysis performed for the jet pump geometries composing the Case Study #2. The results show a maximum efficiency near 30%, instead of the 40% value shown by some geometries included in the Case Study #1. Thus, the results for the Case Study #2 allow one to infer that the adopted mixing throat length was too long, thus giving rise to extra energy losses. That ultimately resulted in smaller values of overall efficiency for such ejector's geometry.

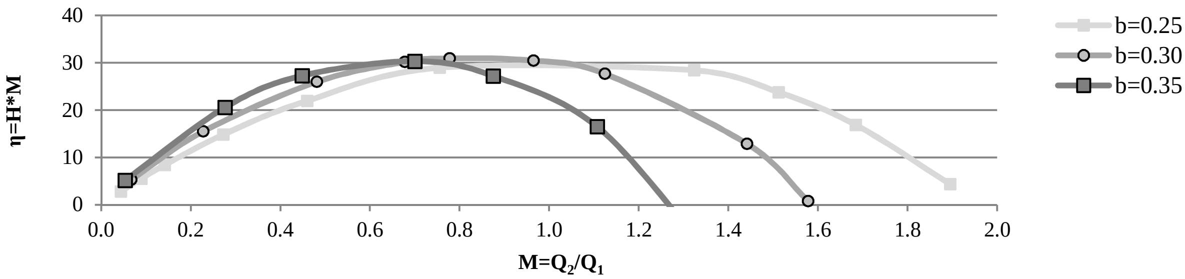

Fig. 7 – Case Study #2 – Efficiency curves (η) as a function of the nozzle-to-throat area ratio

Fig. 8 presents the dimensionless head curves for the three jet pump geometries composing the Case Study #2. Another result is that too long throats yield a lower dimensionless head value, *H*, reducing the jet pump capacity to handle the secondary fluid. It can be observed that the best efficiency point to the Geom4 (*b*=0.3) in Case Study #1 occurs at M=0.95 whereas in Geom9 (b=0.3) in Case Study #2 the best efficiency occurs at M=0.78

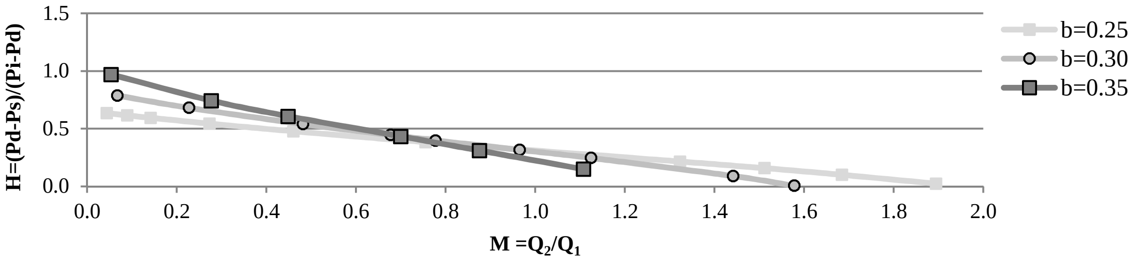

Fig. 8 – Case Study #2 – Dimensionless head curves (H) as a function of the nozzle-to-throat area ratio

The Case Study #3 is composed by a set of five geometries. The difference amongst the five referred geometries is given by different throat length values that vary from 6.5 to 40 throat diameters as shown in the Tab. 2. The main objective for this case of study was to investigate the influence of the throat length in the jet pump efficiency.

Table 2 – Jet Pump Parameters of Study - Case #3

	b	**Φ_n (10^{-2} m)**	**L_{th}**
Geom11	0.25	1.88	$6.5\Phi_{th}$
Geom12	0.25	1.88	$10\Phi_{th}$
Geom13	0.25	1.88	$20\Phi_{th}$
Geom14	0.25	1.88	$30\Phi_{th}$
Geom15	0.25	1.88	$40\Phi_{th}$

The results for the Case Study #3 are shown in Fig. 9 and Fig. 10. It was observed that the maximum jet pump efficiency occurs for a throat length equal to 10 times the throat diameter value. In Fig. 9, the shortest throat length in the referred Case Study #3 could not reach the maximum efficiency value. That suggests that most likely the fluid mixture was not sufficiently homogenous at this spot of the throat length. In the Fig. 10, it is possible to observe that for the highest throat length value, the dimensionless head is lower, which indicates that a too long throat leads to a higher pressure drop. Clearly, if a *maximum maximorum* efficiency value is sought, a finer analysis in the interval of 6.5 to 20 throat diameters for the throat length value would have to be conducted.

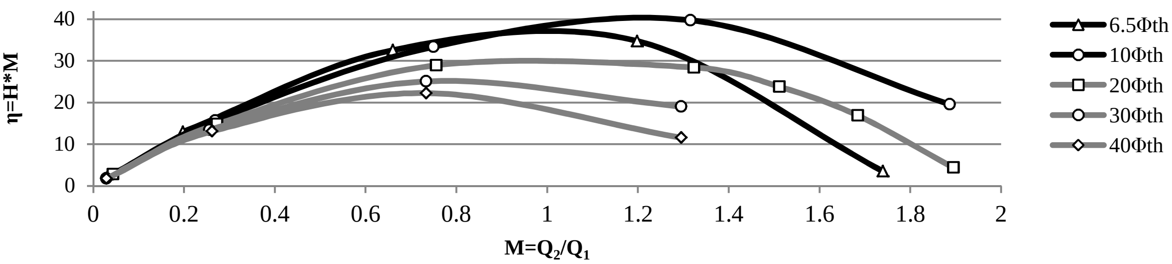

Fig. 9 – Case Study #3 – Efficiency curves (η) as a function of throat length

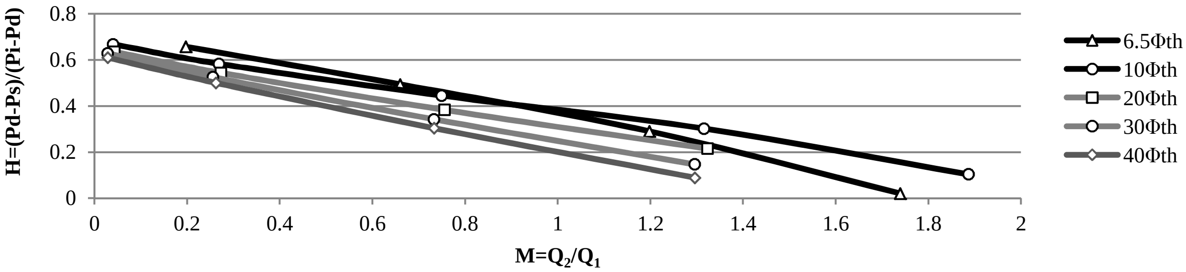

Fig. 10 – Case Study #3 – Dimensionless head (H) as a function of throat length

5. CONCLUSIONS

The two-dimensional CFD model developed for a LJL showed a good agreement with experimental data of Sanger (1970), particularly for low mass flowrate ratio (M). For the best efficiency point and for the high M values, the results showed that deviations between experimental data and CFD results are less than 5%. Thus, the two-dimensional CFD geometry was found to be a valid resource to estimate the LJL efficiency, since it allows different geometry tests with meaningful results in a way that is faster and cheaper than experimental evaluation.

The computational tool also lets one to know the behaviour for the pressure and velocity fields inside the ejector's regions. These results also allow predicting the cavitation phenomenon occurrence and gives insights to the optimization of the key design parameter values for the ejector's concept, design and subsequent construction.

The results obtained by CFD showed good agreement with jet pump efficiency trends found in the literature. The studied cases allowed to confirm the current ejector's design practices, as the one that indicate the nozzle-to-throat area ratio (b) as equal to 0.3 in order to reach the peak jet pump efficiency. It could also be observed that for low nozzle-to-throat area ratio values more fluid can be pumped. Besides, the maximum head is higher for the low nozzle-to-throat area ratio values. In addition, it was shown that there is an optimum length for the ejector's throat region. If such length is shorter than the optimum one, lack of homogenization in the fluid mixture leads to a lower pressure recovery. If such length is longer than the optimal one, extra losses occur in such long throat, also leading to a lower pressure recovery.

When applied to water jet pumps, the good results obtained with the developed methodology seem to indicate that it has a sufficient potential to be equally applied to jet pumps where the primary fluid is a liquid hydrocarbon and the secondary a gas and/or a gas-liquid hydrocarbon mixture, provided that proper modelling treatment for those particular types of fluids and flows be incorporated into the developed methodology.

6. ACKNOWLEDGEMENTS

Authors are thankful to PETROBRAS for the financial support and NUEM (UTFPR) for the technical support.

7. REFERENCES

ANSYS CFX-Solver. Theory Guide. 2013a. ANSYS, Inc.

ANSYS ICEM CFD. User's Manual. 2013b. ANSYS, Inc.

Bird, R. B., Stewart, W. E., Lightfoot, W. E. 2002. *Transport Phenomena*, 2nd edition. John Wiley & Sons, New York.

Baohua, J., 1985. *Behavior of Hydraulic Jet Pumps.* Ph.D. Dissertation. The University of Tulsa, Tulsa.

Cruz, G., 2006. *Simulação Numérica do Escoamento Turbulento em Bomba Ejetora*. M.Sc. Thesis, Aeronautical Technology Institute, São José dos Campos.

Cunningham, R. G., Hansen A. G., Na, T. Y. 1970. "Jet Pump Cavitation". *ASME Journal of Basic Engineering*, Vol.95, p. 483-492.

Cunningham, R. G. 1995. "Liquid Jet Pumps for Two-Phase Flows." *ASME Journal of Fluids Engineering*, Vol. 117, p. 309-316.

Cunningham, R.G. 2001. *Jet Pump Theory*. In *Pump Handbook*, third edition, ed. I. J. Karassik, J. P. Messina, P. Cooper, et al, Chap. 4, Sec. 4.1. McGraw-Hill, 3rd edition.

Fretwell, J. 2006. Hydraulic Pumping in Oil Wells. In *Petroleum Engineering Handbook*, vol. IV, 1st edition, ed. J. D. Clegg, et al. Chap. 14, SPE.

Jumpeter, A.M. 2001. *Jet Pump Applications*. In *Pump Handbook*, third edition, ed. I. J. Karassik, J. P. Messina, P. Cooper, et al, Chap. 4, Sec. 4.2. McGraw-Hill, 3rd edition.

Yapici, R., Aldas, K. 2013. "Optimization of Water Jet Pumps Using Numerical Simulation." *Journal of Power and Energy*, Vol. 227, p. 1-12.

Yule, A. J., Damou, M. and Kostopoulos, D. 1993. "Modeling Confined Jet Flow". *International Journal of Heat and Fluid Flow*, Vol. 14, p. 10-,17.

Launder, B. E., Spalding, D. B. 1973. "The Numerical Computation of Turbulent Flows". *Computer Methods in Applied Mechanics and Engineering*, Vol. 3, p. 269-289.

Lima Neto, I. E. 2011. "Maximum Suction Lift of Water Jet Pumps". *Journal of Mechanical Science and Technology*, Vol. 25, p. 391-394.

Nallasamy, M. 1985. "A Critical Evaluation of Various Turbulence Models as Applied to Internal Fluid Flows." *NASA Technical Paper*, n. 2474.

Noronha, F. A. F., França, F. A. and, Alhanati, F. J. S. 1998. "Improved Two-Phased Model for Hydraulic Jet Pumps". SPE Journal, Vol. 3, p.227-231.

Pope, A. B. 1978. "An Explanation of the Turbulent Round-Jet/Plane Jet Anomaly". *AIAA JOURNAL*, Vol. 16, p. 279-281.

Sanger, N. L. 1970. "An Experimental Investigation of Several Low-Area-Ratio Water Jet Pumps". *Journal of Basic Engineering*, Vol. 92, p. 11-19.

8. RESPONSIBILITY NOTICE

The authors are the only responsible for the printed material included in this paper.